改善が認められた。

2）SBMA に対するリュープロレリン酢酸塩の第Ⅱ相臨床試験

SBMA は緩徐進行性の疾患で、病態を反映するバイオマーカーが確立されていないため、まずサロゲートエンドポイントとなりうる臨床評価指標を探索した。とくに予後に直結する球麻痺の解析方法として嚥下造影に注目し、空間的・時間的解析による嚥下機能の定量化を検討した。その結果、食道入口部開大時間が患者の重症度と最もよく相関し、再現率の高い優れたマーカーであることが明らかとなった。そこで、運動機能スコア（ALSFRS-R）を主要評価項目、食道入口部開大時間などを副次的評価項目とする第Ⅱ相臨床試験をデザインし、SBMA 患者に対するリュープロレリン酢酸塩の治療効果を検討した。50 例の被験者を対象に試験を行ったところ、48 週間のプラセボ対照比較試験ではリュープロレリン酢酸塩による血清テストステロンの有意な低下、血清 CK の有意な低下、陰嚢皮膚における 1C2（抗ポリグルタミン抗体）陽性細胞数の有意な減少、および嚥下造影における食道入口部開大時間の有意な改善が認められ、その後の継続試験ではリュープロレリン酢酸塩の長期投与（144 週）により運動機能スコア（ALSFRS-R）の悪化が有意に抑制されることが明らかとなった（Banno et al., ***Ann Neurol*** 2009）。有害事象は前立腺癌患者に対する臨床試験の成績と比べ明らかな差は乏しかった。

D. 考察

SBMA などの神経変性疾患の病態の根本は、異常な構造を持つ変異蛋白質が、生態の防御機構を凌駕して細胞内に蓄積することと考えられている。このため、蛋白質の品質管理機構であるユビキチン-プロテアソーム系と分子シャペロンを活性化することで変異蛋白質の毒性を軽減できれば、神経変性の病態を阻止できると予想される。今回の検討では、SBMA のモデルマウスではユビキチン-プロテアソーム系の機能が維持されていること、およびその機能を活性化する薬物治療が、マウスの運動機能や病理所見を改善することが示された。ユビキチン-プロテアソーム系は SBMA をはじめとする神経変性疾患の治療標的として極めて重要と考えられる。

一方、我々のこれまでの検討により、テストステロンの分泌阻害が変異アンドロゲン受容体の核内凝集を強力に阻害することが明らかとなっていたが、リュープロレリン酢酸塩の第Ⅱ相臨床試験においても、病因蛋白質の凝集阻害効果が示された。さらに、リュープロレリン酢酸塩の長期投与により、患者の運動機能が改善する傾向も示された。現在、この結果を第Ⅲ相大規模臨床試験において検証しているところである。

E. 結論

今回の検討により、17-DMAG がユビキチン-プロテアソーム系を介して変異アンドロゲン受容体の分解を促進し、SBMA モデルマウスにおける神経変性過程を阻止することが示された。また、テストステロンの分泌を阻害することにより、SBMA 患者においても変異アンドロゲン受容体の核内凝集が阻害され、神経障害の進行が抑制される可能性が示唆された。

F. 健康危険情報　なし

G. 研究発表

1．論文発表

1) Banno H, **Katsuno M***, Suzuki K, Tanaka F. Sobue G*. Neuropathology and therapeutic intervention in spinal and bulbar muscular atrophy. ***Int J Mol Sci*** [in press]. *corresponding authors.

2) Morozumi S, Kawagashira Y, Iijima M, Koike H, Hattori N, **Katsuno M**, Tanaka F, Sobue G. Intravenous immunoglobulin treatment for painful sensory neuropathy associated with

Sjögren's syndrome. ***J Neurol Sci*** 279: 57-61, 2009.

3) **Katsuno M***, Adachi H, Sobue G*. Getting a handle on Huntington's disease: the case for cholesterol. ***Nat Med.*** 15: 253-254, 2009. *corresponding authors.

4) Banno H, **Katsuno M***, Suzuki K, Takeuchi Y, Kawashima M, Suga N, Takamori M, Ito M, Nakamura T, Matsuo K, Yamada S, Oki Y, Adachi H, Minamiyama M, Waza M, Atsuta N, Watanabe H, Fujimoto Y, Nakashima T, Tanaka F, Doyu M, Sobue G*. Phase 2 trial of leuprorelin in patients with spinal and bulbar muscular atrophy. ***Ann Neurol.*** 65: 140-150, 2009. *corresponding authors.

5) Watanabe H, Hirayama M, Noda A, Ito M, Atsuta N, Senda J, Kaga T, Yamada A, **Katsuno M**, Niwa T, Tanaka F, Sobue G. B-type natriuretic peptide and cardiovalvulopathy in Parkinson disease with dopamine agonist. ***Neurology*** 72: 621-626, 2009.

6) Senda J, Ito M, Watanabe H, Atsuta N, Kawai Y, **Katsuno M**, Tanaka F, Naganawa S, Fukatsu H, Sobue G. Correlation between pyramidal tract degeneration and widespread white matter involvement in amyotrophic lateral sclerosis: A study with tractography and diffusion-tensor imaging. ***Amyotroph Lateral Scler.*** [in press].

7) Suzuki K, **Katsuno M**, Banno H, Sobue G. Pathogenesis-targeting Therapeutics for Spinal and Bulbar Muscular Atrophy (SBMA). ***Neuropathology*** [in press].

8) Tokui K, Adachi H, Waza M, **Katsuno M**, Minamiyama M, Doi H, Tanaka K, Hamazaki J, Murata S, Tanaka F, Sobue G. 17-DMAG ameliorates polyglutamine-mediated motor neuron degeneration through well-preserved proteasome function in a SBMA model mouse. ***Hum Mol Genet.*** 18: 898-910, 2009.

9) Takeuchi Y, **Katsuno M***, Banno H, Suzuki K, Kawashima M, Atsuta N, Ito M, Watanabe H, Tanaka F, Sobue G*. Walking capacity evaluated by the 6-minute walk test in spinal and bulbar muscular atrophy. ***Muscle Nerve.*** 38: 964-971, 2008. *corresponding authors

10) Iijima M, Koike H, Hattori N, Tamakoshi A, **Katsuno M**, Tanaka F, Yamamoto M, Arimura K, Sobue G.Prevalence and incidence rates of chronic inflammatory demyelinating polyneuropathy in the Japanese population. ***J Neurol Neurosurg Psychiatry.*** 79: 1040-1043, 2008.

11) **Katsuno M***, Banno H, Suzuki K, Takeuchi Y, Kawashima M, Adachi H, Tanaka F, Sobue G*. Molecular Genetics and Biomarkers of Polyglutamine Diseases. ***Current Mol Med.*** 8: 221-234, 2008. *corresponding authors

12) Suenaga M, Kawai Y, Watanabe H, Atsuta N, Ito M, Tanaka F, **Katsuno M**, Fukatsu H, Naganawa S, Sobue G. Cognitive impairment in spinocerebellar ataxia type 6. ***J Neurol Neurosurg Psychiatr.y*** 79: 496-499, 2008.

13) Suzuki K, **Katsuno M**, Banno H, Takeuchi Y, Atsuta N, Ito M, Watanabe H, Yamashita F, Hori N, Nakamura T, Hirayama M, Tanaka F, Sobue G. CAG repeat size correlates to electrophysiological motor and sensory phenotypes in SBMA. ***Brain*** 131: 229-239, 2008.

2．学会発表

1. Adachi H, Tokui K, Waza M, **Katsuno M**, Minamiyama M, Doi H, Tanaka F, Sobue G. An oral Hsp90 inhibitor ameliorates phenotypes of the spinal and bulbar muscular atrophy transgenic mouse model. Neuroscience 2009, Washington DC, USA, Nov 15-19, 2008.

2. **Katsuno M**, Kawashima M, Banno H, Suzuki K, Takeuchi Y, Suga N, Adachi H, Tanaka F, Sobue G: Skeletal muscle involvement in spinal and bulbar muscular atrophy. The 19th

International Symposium on ALS/MND. Birmingham, UK, Nov 3-5, 2008.

H. 知的財産権の出願・登録状況

なし

厚生労働省科学研究費補助金（こころの健康科学研究事業）
分担研究報告書

運動ニューロン変性に関わる分子の同定と病態抑止治療法の開発

研究分担者：田中　啓二　　東京都臨床医学総合研究所・所長代行

研究要旨
プロテアソームは非分裂細胞であるニューロンにおけるタンパク質の品質管理に重要であることが示唆されているが、これまでは阻害剤を用いた in vitro の研究が主流であった。我々は、最近、プロテアソームの分子集合に係わる因子として Proteasome Assembling Chaperone（PAC）1-4 を発見した。本研究では、PAC1 の欠損マウスを作出し、プロテアソームの量を徐々に削減した場合におけるニューロンの動態について解析することを目指した。そのために我々は PAC1 条件付き遺伝子欠損マウスを作出し、多面的な解析を行った。PAC1 全身欠損マウスは早期胎生致死となったことから、シャペロン依存的なプロテアソームの分子集合機構がマウスの個体発生に必須であることが判明した。さらに中枢神経系特異的に PAC1 を欠損したマウスを作出したところ、プロテアソームの低下と並行して、平衡感覚・発育異常が見られることに加え、大脳皮質、小脳皮質において特徴的な層状構造の形成が阻害されるという reeler、yotari マウスに酷似した様態を示すことが明らかとなった。現在、プロテアソームのレベル低下が様々なニューロンに及ぼす影響についての詳細に解析中である。

A. 研究目的

プロテアソームはユビキチン化されたタンパク質を選択的に分解する酵素であり、細胞内のタンパク質バランスの維持に中心的な役割を担っている。活性型プロテアソーム(26S プロテアソーム)はコアとなる 20S プロテアソーム（触媒機能を司どる）と制御因子である 19S RP（regulatory particle）から構成される 60 個以上ものサブユニットが集合した約 2.5 MDa の分子量をもつ巨大な多分子複合体である。しかし、どのようにしてこれほどまでの多くのサブユニットが常に整然と並びこの複合体を作り上げているのかは、長らく謎であった。

真核生物の 20S プロテアソームは$\alpha_{1-7}\beta_{1-7}$（ハーフプロテアソーム）の 2 層のリングが 2 回軸対称により四層リングの複合体（$\alpha_{1-7}\beta_{1-7}\beta_{1-7}\alpha_{1-7}$）を形成しており、その分子集合過程は①αリングの形成、②αリングへのβサブユニット結合によるハーフプロテアソームの形成、③ハーフプロテアソーム 2 分子の会合による 20S プロテアソーム形成の順に行われている。この過程において我々は、①のαリング形成時にシャペロンタンパク質 PAC1-PAC2[1] 及び PAC3-PAC4 複合体(酵母では Pba1-Pba2、Dmp1/Pba4-Dmp2/Pba3 複合体)[2, 3] が関与し、②、③の過程ではもう一つのシャペロンである Ump1 が関与していることを突き止めた。さらにβリング形成にはβサブユニットのプロペプチドや C-端の延長鎖(これらは分子内シャペロンと呼ばれている)が重要な役割を担っていることを明らかにした[4]。このように真核生物の 20S プロテアソームの複合体形成は、複数の分子シャペロンによって支援された逐次的多段階機構で行われることが判明した（詳細は総説 5 & 6 を参照)。これらの研究によりプロテアソームが、正しく複合体を構築するためには、各構成サブユニットのホモオリゴマー形成、誤った部位への結合、不完全な複合体形成等の阻止が必須であり、シャペロンタンパク質はこれらを効率よく解決する合理的なシステムであることが分かってきた。

そこで本研究では、PAC 依存性のプロテアソームの形成活性を調節して、細胞内のプロテアソームの量を制限することが可能なマウスを作出することを目指した。作出した PAC1 遺伝子を条件的に不能にするマウスを用いて、中枢神経系細胞の機能におけるプロテアソームの役割の解明を行った。

B. 研究方法

最初に Flip-FRT & cre-lox システムを

利用した条件付き PAC1 欠損マウスを作出した。この変異マウスと種々のプロモーター制御下 Cre リコンビナーゼ発現トランスジェニックマウス（Tg）と掛け合わせることによって PAC1 欠損マウスを作出することが可能になった。今回は Cre リコンビナーゼを全身および神経幹細胞特異的に発現させ PAC1 を欠損させることで解析を行った。全身発現にはアデノウイルス EIIa プロモーター、神経幹細胞発現にはマーカー分子として知られる Nestin のプロモーターを利用したトランスジェニックマウスを用いた。その他の解析方法としては、形態学的な手法とプロテアソームの解析を中心とした生化学的な手法を駆使して行った。

（倫理面への配慮）
本年度の研究は、主として培養細胞およびマウスを用いた基礎的研究およびリコンビナントタンパク質を用いた生化学的・構造生物学的研究である。従って、これらの実験の実施には、倫理面への配慮は不要であった。

C. 研究結果
酵母 Dmp1-Dmp2 複合体の立体構造

20S プロテアソームの分子集合に関与する Dmp1-Dmp2 複合体は出芽酵母の非必須遺伝子破壊株ライブラリーからアミノ酸アナログ感受性となる出芽酵母変異株を探索することによって同定した。その後の解析から、この複合体が直接結合する分子がプロテアソームのα5 サブユニットであること、さらに完成した 20S プロテアソーム複合体には Dmp1-Dmp2 複合体が含まれていないことから、この複合体が高次構造形成に関与するシャペロン因子であることを明らかにした。本年度、我々は Dmp1-Dmp2 複合体と Dmp1-Dmp2 とα5 サブユニット複合体のX線結晶構造解析を行い、立体構造を決定した（名古屋市立大学・水島恒裕／加藤晃一らとの共同研究）。興味深いことに Dmp1 と Dmp2 の立体構造は一次構造上有意な相同性を示さないにもかかわらず非常によく似ていた。さらに Dmp1-Dmp2-α5 サブユニット複合体の立体構造解析から Dmp1-Dmp2 はαリングにβリング側から結合し二量体の境界領域でα5 サブユニットを認識しており、その結合部位はβサブユニットよりリングの内側に位置することも判明した。またβサブユニット側からαリングに結合しているため、βリングと Dmp1-Dmp2 が共存できないことが明らかとなった。次に Dmp1-Dmp2 とαリングの複合体モデル作出により、Dmp1-Dmp2 がα4,α5,α6 とも結合面を持つプロテアソーム中間体モデルを提案した。その結果、Dmp1-Dmp2 は 20S プロテアソームの複合体構築においてβ4 がαリングに結合する際にプロテアソーム中間体から解離することが示された[3]。

哺乳類 20S プロテアソームの触媒機能を司るβリングの形成経路

βリングの形成機構の解析は 20S プロテアソームを構成する各々のβサブユニットを siRNA（small interfering RNA）によりノックダウンすることでβリングの形成を途中段階で阻害し、それにより生じた中間状態を解析する方法で行った。その結果、βサブユニットのαリングに対する結合は決まった順序で行われており、αリングにβ2,3,4,5,6 の順番で結合することが明らかになった。さらにβ1 はβ2,3 が結合した後であればいつでも結合できること、最後にβ7 が結合しハーフプロテアソームを完成することが判明した。このプロセスにおいて、PAC1-PAC2、PAC3-PAC4 はαリング形成時に結合しており、一方、Ump1 は哺乳類では酵母の場合と異なりβ2 と同時にαリングに結合することが判明した（酵母では Ump1 がハーフプロテアソームの二量体化に関与することが知られている）。PAC3-PAC4 はβ3 の結合により解離し、Ump1 はハーフプロテアソームから 20S プロテアソームを形成する際に分解される。さらに PAC1-PAC2 は 20S プロテアソームが完成した後で分解されることが明らかになった[4]。

全身 PAC1 欠損マウスの解析

PAC1 全身欠損マウスについてであるが、このマウスはヘテロ接合体の場合はほぼ外見上野生型と変わらなかった。ホモ接合体に関しては出生後の遺伝子型解析で確認することができなったため胎生致死であることが推察された。胎児期における異常を解析するために切片を作出し形態学的な解析を試みた。その結果 E6.5、E7.5 においてメンデルの法則に従って胎児の消失が起きているものが確認できた。またそれらは E6.0 における抗 PAC1 抗体による免疫染色から PAC1 が完全に欠損した個体であることを確認でき

た。これらのことからPAC1の全身欠損マウスは着床後早期の発達異常による胎生致死となることが明らかになった(論文作成中)。

中枢神経系PAC1欠損マウスの解析

次に神経幹細胞Nestinプロモーター制御下でPAC1を欠損させたマウスの解析を行った。こちらもヘテロ接合体では野生型と表現系は変わらなかった。ヘテロ接合体では生後1週頃から発育異常、平衡感覚・歩行異常が顕著になり、生後3週で死亡する(咀嚼、嚥下運動機能低下による栄養摂取の障害によるものと考えられる)。3週齢の大脳、小脳のホモジネートライセートをグリセロール密度勾配遠心により分画し20Sプロテアソーム、26Sプロテアソームのペプチダーゼ活性を測定すると20Sプロテアソームに関してはほぼ完全に消失し、26Sプロテアソームに関しては2ー3割近くまで減少していた。形態学的にみると特に小脳における特徴的な層構造形成が顕著に阻害されていることが分かった。経時的な解析を行うと、このPAC1ホモ欠損マウスの小脳は外見上、出生直後から発達が進んでいないことが分かった。さらに生後に増殖・移動を繰り返し小脳の大部分を占めるようになる顆粒球の異常が原因ではないかと考え、核酸アナログであるBrdUの取り込み実験を行い解析すると小脳において顆粒球前駆細胞または顆粒球の増殖する割合がホモ欠損体では極度に低下していることが観察された。またもう一つの知見としては大脳、小脳において同程度のプロテアソームのペプチダーゼ活性が低下しているにもかかわらず、3週齢ホモ欠損体の特に小脳では不特定複数のユビキチン強陽性細胞が確認された。これは2週齢以降の小脳から確認できた(論文作成中)。

D. 考察

今回の遺伝子改変(PAC1欠損)マウスを用いた研究によりプロテアソーム複合体の存在が生理学的に重要であることが改めて示された。全身欠損マウスの解析では胎児期の初期発達に必須であることが示唆された。また神経幹細胞特異的欠損マウスの解析においては小脳の形成障害という興味深い現象を引き起こすことを観察でき、プロテアソームの形成、活性の低下とマウスを個体とした生理学的な異常の2つの関係性を明確に示すことができた。しかし、今回の小脳における現象はプロモーターとして用いたNestinの発現時期特異性、プロテアソームの活性減弱スピード、小脳の特徴的な発達過程等を複合的に考えることが必要であり、以上の要因を考慮するとプロテアソームがほかの脳組織に比して小脳の形成に選択的に関与しているとは断言できない。

今回、細胞の種類、時期によってプロテアソームもしくはユビキチンープロテアソームシステムへの依存性が変化することが示唆されたことで個体におけるプロテアソームの役割を今後解釈していく際に重要な知見が得られたのではないかと考えている。

E. 結論

PAC1全身欠損マウスは、着床後早期の発達異常による胎生致死となり、シャペロン依存性のプロテアソームの形成がマウスの個体発生に重要であることが初めて明らかになった。次に神経幹細胞で発現しているNestinのプロモーター制御下でPAC1を欠損させたマウスを作出し、ニューロンの挙動を解析した。中枢神経系特異的PAC1欠損マウスは、生後1週頃から発育異常、平衡感覚・歩行異常が顕著になり、生後3週で死亡した。形態学的にみると大脳皮質や小脳における特徴的な層構造形成が顕著に阻害されていることが分かった。

F. 健康危険情報

無し。

G. 研究発表

1. 論文発表

(1) Hirano, Y., Hendil, K.B., Yashiroda, H., Iemura, S., Nagane, R., Hioki, Y., Natsume, T., Tanaka, K., and Murata, S. (2005) A heterodimeric complex that promotes the assembly of mammalian 20S proteasomes, **Nature** 437, 1381-1385.

(2) Hirano, Y., Hayashi, H., Iemura, S., Hendil, K.B., Niwa, S., Kishimoto, T., Natsume, T., Kasahara, M., Tanaka, K., and Murata, S. (2006) Cooperation of multiple chaperones required for the assembly of mammalian 20S proteasomes.

Mol Cell 24, 977-984.

(3) Yashiroda, H*., Mizushima, T.*, Okamoto, K., Kameyama, T., Hayashi, H., Kishimoto, T., Kasahara, M., Kurimoto, E., Sakata, E., Suzuki, A., Hirano, Y., Murata , S., Kato, K., Yamane, T., and Tanaka, K. (2008) Crystal structure of a chaperone complex that contributes to the assembly of yeast 20S proteasomes. **Nature Struct. Mol. Biol**. 15, 228 – 236.

(4) Hirano, Y., Kaneko, T., Okamoto, K., Bai, M., Yashiroda, H., Furuyama, K., Kato, K., Tanaka, K., and Murata, S. (2008) Dissecting β-ring assembly pathway of the mammalian 20S proteasome. **EMBO J**. 27, 2204-2213.

(5) Murata, S., Yashiroda, H., and Tanaka, K. (2009) Molecular mechanisms of proteasome assembly. **Nature Rev Mol Cell Biol** 10, 104-115.

(6) Tanaka, K. (2009) The proteasome: Overview of structure and functions. **Proc. Jpn. Acad. Ser B Phys Biol Sci**. 85, 12-36.

2．学会発表

田中啓二：Protein Degradation and Neurodegenerative Diseases. Neuroscience 2008 第31回日本神経科学大会.特別講演。July 10, 2008（東京フォーラム）東京.

田中啓二：タンパク質分解と病態生理学 (Proteolysis and Pathophysiology). 第２回 Diabetes Leading-edge Conference：静岡県沼津市淡島ホテル（平成２０年８月９日）静岡

Keiji Tanaka：The Novel Thymoproteasome Regulates Development of $CD8^+$ T Cells. 33rd FEBS Congress & 11th IUBMB Conference （Symposium on the ubiquitin-proteasome system）Peace and Friendship Stadium, June 30, 2008, Athens,Greece.

Keiji Tanaka：Unexpected encounter with immunity during my proteasome study. Japan-German Immunology Seminar 2008 ： Immune Regulation in Health and Disease. (November 3-6, 2008) Fukuoka, Japan

H. 知的財産権の出願・登録状況

1．特許取得

無し

2．実用新案登録

無し

3．その他

無し

III. 研究成果の刊行に関する一覧表

研究成果の刊行に関する一覧表

祖父江　元　名古屋大学大学院医学系研究科神経内科学教授
田中　章景　名古屋大学大学院医学系研究科神経内科学准教授
勝野　雅央　名古屋大学高等研究院　特任講師

雑誌

発表者氏名	論文タイトル名	発表誌名	巻号	ページ	出版年
Suzuki K, Katsuno M, Banno H, Sobue G.	Pathogenesis-targeting Therapeutics for Spinal and Bulbar Muscular Atrophy (SBMA).	**Neuropathology**	in press		
Banno H, Katsuno M, Suzuki K, Tanaka F. Sobue G.	Neuropathology and therapeutic intervention in spinal and bulbar muscular atrophy.	**Int. J. Mol. Sci.**	in press		
Senda J, Ito M, Watanabe H, Atsuta N, Kawai Y, Katsuno M, Tanaka F, Naganawa S, Fukatsu H, Sobue G.	Correlation between pyramidal tract degeneration and widespread white matter involvement in amyotrophic lateral sclerosis: A study with tractography and diffusion-tensor imaging.	**Amyotroph. Lateral Scler.**	in press		
Katsuno M, Adachi H, Sobue G.	Getting a handle on Huntington's disease: the case for cholesterol.	**Na.t Med.**	15	253-254	2009
Young JE, Garden GA, Martinez RA, Tanaka F, Sandoval CM, Smith AC, Sopher BL, Lin A, Fischbeck KH, Ellerby LM, Morrison RS, Taylor JP, La Spada AR.	Polyglutamine-expanded androgen receptor truncation fragments activate a Bax-dependent apoptotic cascade mediated by DP5/Hrk.	**J. Neurosci.**	29	1987-1997	2009
Morozumi S, Kawagashira Y, Iijima M, Koike H, Hattori N, Katsuno M, Tanaka F, Sobue G.	Intravenous immunoglobulin treatment for painful sensory neuropathy associated with Sjögren's syndrome.	**J. Neurol. Sci**	279	57-61	2009

Banno H, Katsuno M, Suzuki K, Takeuchi Y, Kawashima M, Suga N, Takamori M, Ito M, Nakamura T, Matsuo K, Yamada S, Oki Y, Adachi H, Minamiyama M, Waza M, Atsuta N, Watanabe H, Fujimoto Y, Nakashima T, Tanaka F, Doyu M, Sobue G.	Phase 2 trial of leuprorelin in patients with spinal and bulbar muscular atrophy.	**Ann. Neurol.**	65	140-150	2009
Tokui K, Adachi H, Waza M, Katsuno M, Minamiyama M, Doi H, Tanaka K, Hamazaki J, Murata S, Tanaka F, Sobue G.	17-DMAG ameliorates polyglutamine-mediated motor neuron degeneration through well-preserved proteasome function in a SBMA model mouse.	**Hum. Mol. Genet.**	18	898-910	2009
Watanabe H, Hirayama M, Noda A, Ito M, Atsuta N, Senda J, Kaga T, Yamada A, Katsuno M, Niwa T, Tanaka F, Sobue G.	B-type natriuretic peptide and cardiovalvulopathy in Parkinson disease with dopamine agonist.	**Neurology**	72	621-626	2009
Takeuchi Y, Katsuno M, Banno H, Suzuki K, Kawashima M, Atsuta N, Ito M, Watanabe H, Tanaka F, Sobue G.	Walking capacity evaluated by the 6-minute walk test in spinal and bulbar muscular atrophy.	**Muscle Nerve**	38	964-971	2008
Iijima M, Koike H, Hattori N, Tamakoshi A, Katsuno M, Tanaka F, Yamamoto M, Arimura K, Sobue G.	Prevalence and incidence rates of chronic inflammatory demyelinating polyneuropathy in the Japanese population.	**J. Neurol. Neurosurg. Psychiatry**	79	1040-1043	2008

Katsuno M, Banno H, Suzuki K, Takeuchi Y, Kawashima M, Adachi H, Tanaka F, Sobue G.	Molecular Genetics and Biomarkers of Polyglutamine Diseases.	**Current Mol. Med.**	8	221-234	2008
Suenaga M, Kawai Y, Watanabe H, Atsuta N, Ito M, Tanaka F, Katsuno M, Fukatsu H, Naganawa S, Sobue G	T Cognitive impairment in spinocerebellar ataxia type 6.	**J. Neurol. Neurosurg. Psychiatry**	79	496-499	2008
Suzuki K, Katsuno M, Banno H, Takeuchi Y, Atsuta N, Ito M, Watanabe H, Yamashita F, Hori N, Nakamura T, Hirayama M, Tanaka F, Sobue G	CAG repeat size correlates to electrophysiological motor and sensory phenotypes in SBMA.	**Brain**	131	229-239	2008

研究成果の刊行に関する一覧表

雑誌　　田中　啓二　　東京都臨床医学総合研究所・所長代行

発表者氏名	論文タイトル名	発表誌名	巻号	ページ	出版年
Murata S, Yashiroda H, Tanaka K.	Molecular mechanisms of proteasome assembly.	***Nat. Rev. Mol. Cell. Biol.***	10	104-115	2009
Tanaka K.	The proteasome: Overview of structure and functions.	***Proc. Jpn. Acad. Ser. B Phys. Biol. Sci.***	85	12-36	2009
Yashiroda H, Mizushima T, Okamoto K, Kameyama T, Hayashi H, Kishimoto T, Kasahara M, Kurimoto E, Sakata E, Suzuki A, Hirano Y, Murata S, Kato K, Yamane T, Tanaka K.	Crystal structure of a chaperone complex that contributes to the assembly of yeast 20S proteasomes.	***Nat. Struct. Mol. Biol.***	15	228 – 236	2008
Hirano Y, Kaneko T, Okamoto K, Bai M, Yashiroda H, Furuyama K, Kato K, Tanaka K, Murata S.	Dissecting b-ring assembly pathway of the mammalian 20S proteasome.	***EMBO J.***	27	2204-2213	2008

Ⅳ. 研究成果の刊行物・別冊

modification technologies have led to a resurgence in interest.

Antisense oligonucleotide therapy is emerging as a promising approach to treat neurodegenerative diseases involving production of a toxic gene product. In a 2006 study of antisense oligonucleotide therapy for familial ALS1, which is caused by mutations in the gene encoding SOD1, Smith *et al.*[11] showed widespread distribution of oligonucleotides to all regions of the brain and spinal cord in rats and nonhuman primates, successful knockdown of SOD1 mRNA and protein and marked neuroprotection in a rat model of ALS1.

Building on this result, this group of researchers—a partnership between academic and industry investigators—recently completed the necessary toxicology work and is in the final phases of applying to the US Food and Drug Administration to start a phase 1 clinical trial. This clinical trial will involve 16–20 subjects with SOD1-mediated ALS1 at six sites throughout the US. Antisense oligonucleotides will be infused into the cerebral spinal fluid (intrathecally) by a small pump inserted into the abdomen and connected to the spinal cord via a small plastic tube. The first administration of antisense oligonucleotides will be given as a single 12 hour infusion, and, if tolerated, will be followed by a continuous one month infusion. This phase 1 trial is thus anticipated to last for four to six months. In the case of SOD1, diminished enzymatic activity or even elimination of the gene in *Sod1*-knockout mice does not produce disease or decrease lifespan[12], suggesting that concerns about concomitant loss of function of the normal allele are probably unwarranted. For these reasons, the outcome of the ALS1 antisense oligonucleotide therapy trial is highly anticipated.

The strategy of silencing genes through the use of antisense oligonucleotides or RNAi holds great promise for treating a host of neurological diseases, as gene dosage alterations and key regulatory genes have been implicated in the pathogenesis of Alzheimer's disease, Parkinson's disease, frontotemporal dementia and other neurodegenerative disorders[13]. In the case of many proteins implicated in neurodegeneration, such as amyloid precursor protein, beta-site amyloid precursor protein–cleaving enzyme and tau, reduction of gene expression should be well tolerated, given the results of studies in mice.

Moreover, the recent RNAi knockdown studies in Huntington's disease show that even genes expected to perform key functions can be subjected to a substantial degree of gene silencing in adults without untoward effects[1]. This finding should encourage investigators to move forward with non-allele–specific gene silencing studies in animal models as a prelude to potential application in humans. Such work could herald a new era for the development of therapies to treat neurodegeneration.

1. McBride, J.L. *et al. Proc. Natl. Acad. Sci. USA* **105**, 5868–5873 (2008).
2. Shao, J. & Diamond, M.I. *Hum. Mol. Genet.* **16**, R115–R123 (2007).
3. Taylor, J.P., Hardy, J. & Fischbeck, K.H. *Science* **296**, 1991–1995 (2002).
4. Yamamoto, A., Lucas, J.J. & Hen, R. *Cell* **101**, 57–66 (2000).
5. Zu, T. *et al. J. Neurosci.* **24**, 8853–8861 (2004).
6. Xia, H. *et al. Nat. Med.* **10**, 816–820 (2004).
7. Cattaneo, E., Zuccato, C. & Tartari, M. *Nat. Rev. Neurosci.* **6**, 919–930 (2005).
8. La Spada, A.R. & Taylor, J.P. *Neuron* **38**, 681–684 (2003).
9. Bonini, N.M. & La Spada, A.R. *Neuron* **48**, 715–718 (2005).
10. Crooke, S.T. *Annu. Rev. Med.* **55**, 61–95 (2004).
11. Smith, R.A. *et al. J. Clin. Invest.* **116**, 2290–2296 (2006).
12. Cleveland, D.W. & Rothstein, J.D. *Nat. Rev. Neurosci.* **2**, 806–819 (2001).
13. Lee, J.A. & Lupski, J.R. *Neuron* **52**, 103–121 (2006).

■ BEDSIDE TO BENCH

The case for cholesterol

Masahisa Katsuno, Hiroaki Adachi & Gen Sobue

Since the first description in 1872 (ref. 1) of Huntington's disease—a hereditary neurodegenerative disease characterized by progressive movement disorder, cognitive decline and psychiatric disturbances—tremendous efforts have been made to cure it. However, no effective therapy exists, except for a few symptomatic treatments, such as tetrabenezine, which attenuates involuntary movement.

A recent clinical study of people with Huntington's disease hints that low concentrations of brain cholesterol may contribute to disease and bolsters the emerging idea that targeting cholesterol metabolism has the potential to be beneficial[2]. The findings dovetail with studies in animals and people suggesting that low amounts of brain cholesterol might play a part in a range of neurodegenerative disorders.

Huntington's disease is one of the devastating neurodegenerative disorders resulting from expansion of a genomic trinucleotide CAG repeat, which encodes a polyglutamine tract in causative proteins. Although the genes encoding these proteins are distinct from one another except for the expanded CAG repeats, polyglutamine-mediated neurodegenerative disorders share salient features, such as a selective loss of neurons within the central nervous system and a slow progression of neurological deficits.

Therefore, the pathophysiology of Huntington's disease is likely to be closely related to that of other polyglutamine diseases. In support of this view, various cell culture and animal studies show that the pathogenic polyglutamine proteins have a propensity to accumulate in neurons and, thereby, trigger several molecular events that lead to neuronal dysfunction and eventual cell death.

For example, it has been suggested that nuclear accumulation of huntingtin, the causative protein of Huntington's disease, impairs transcription by interfering with the activity of transcription factors[3]. It is, therefore, not surprising that the abnormal accumulation of pathogenic polyglutamine proteins is a major target of therapeutic interventions[4]. Mitochondrial dysfunction, axonal transport disruption and oxidative stress have also been implicated in the molecular mechanisms of polyglutamine diseases. Thus, the quantitative assessment of these cellular events is important for the development of therapy as well as for the evaluation of disease progression.

In a recent clinical study, Leoni *et al.*[2] showed that concentrations of 24S-hydroxycholesterol, a cholesterol metabolite produced in the brain, are substantially decreased in the plasma of people with Huntington's disease compared with healthy subjects. They found that this decrease in 24S-hydroxycholesterol parallels the decrease in volume of the caudate, a brain region affected in the disease, observed from before onset to

Masahisa Katsuno, Hiroaki Adachi and Gen Sobue are in the Department of Neurology, Nagoya University Graduate School of Medicine, 65 Tsurumai-Cho, Showa-ku, Nagoya 466-8550, Japan. Masahisa Katsuno is also at the Institute for Advanced Research, Nagoya University, Furo-cho, Chikusa-ku, Nagoya 464-8601, Japan.
e-mail: sobueg@med.nagoya-u.ac.jp or ka2no@med.nagoya-u.ac.jp

early stages of Huntington's disease[4].

24S-hydroxycholesterol helps maintain constant levels of brain cholesterol, which is required for proper neuronal activity. Brain cholesterol is metabolically separated from other pools by the blood-brain barrier. By virtue of this tight segregation, cholesterol metabolism within the brain is isolated from any changes in the circulating amounts of lipids that result from diet or medication. Brain cholesterol does not come from the blood but is synthesized locally, suggesting the need for elaborate cellular machinery to remove cholesterol from the brain to the circulation to maintain the steady-state level of brain cholesterol. This intrabrain metabolism of cholesterol is ensured by cholesterol 24-hydroxylase, a cytochrome P450 enzyme (encoded by *CYP46A1*) that catalyzes the conversion of cholesterol to 24S-hydroxycholesterol. Whereas unmodified cholesterol does not diffuse into the bloodstream, 24S-hydroxycholesterol crosses the blood-brain barrier.

The study by Leoni *et al.*[2] strongly indicates that the level of plasma 24S-hydroxycholesterol is a promising biomarker that reflects the early progression of neurodegeneration in the disease. Although there is a possibility that the decrease in 24S-hydroxycholesterol simply reflects the reduction in the number of metabolically healthy neurons within affected brain areas, a reasonable hypothesis is that the proper metabolism of cholesterol is impaired in the brains of people with Huntington's disease.

Other studies support this view. For instance, pathogenic huntingtin proteins have been shown to diminish brain cholesterol by inducing transcriptional downregulation of a series of sterol regulatory element–regulated gene products that are essential for cholesterol biosynthesis[5]. A decreased amount of 24S-hydroxycholesterol has also been reported in a transgenic mouse model of Huntington's disease[6]. These human and animal studies strongly underscore the need to exploit pharmacological correction of brain cholesterol metabolism as a promising therapeutic strategy against Huntington's disease.

Dysregulation of cholesterol could affect the nervous system in multiple ways. Cholesterol is an essential component of mammalian cellular membranes, being required for proper permeability and fluidity. Although the human brain represents only two percent of total body mass, it is the most cholesterol-rich organ in the body, accounting for approximately one-fourth of total body cholesterol. Brain cholesterol is not only a major component of myelin and cell membranes but also necessary for a number of normal brain functions, such as membrane trafficking, signal transduction, neurotransmitter release and synaptogenesis.

The tendrils of cholesterol metabolism are also far reaching. The process of synthesizing 24S-hydroxycholesterol generates nonsterol isoprenoids, geranylgeranyl pyrophosphate and farnesyl pyrophosphate, which activate small GTP-binding proteins such as Rho (Fig. 1). Given that Rho family GTPases control neuronal activities and survival through the regulation of neurite outgrowth, cellular polarity, axonal navigation and synapse formation, cholesterol 24-hydroxylase would seem to play an important part in the maintenance of brain functions. This hypothesis has been tested in the *Cyp46a1*-knockout mouse, which shows a learning defect owing to the decreased metabolism of brain cholesterol[7]. Moreover, geranylgeraniol, a precursor of geranylgeranyl pyrophosphate, improves hippocampal long-term potentiation in this mouse model[7].

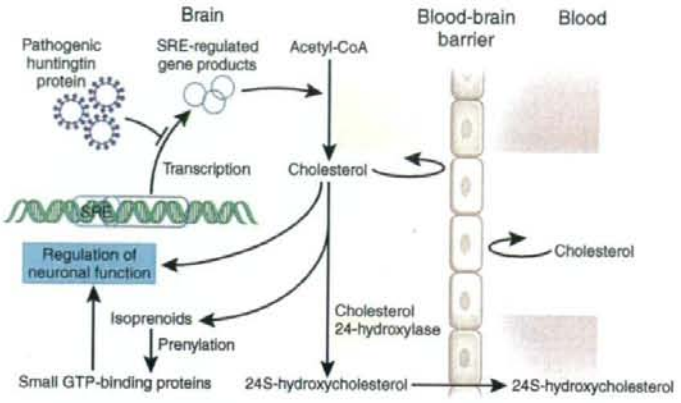

Figure 1 Disrupted cholesterol metabolism may contribute to neurodegeneration in Huntington's disease. Cholesterol is synthesized from acetyl-CoA in adult brain. Brain-generated cholesterol does not cross the blood-brain barrier, but 24S-hydroxycholesterol, an oxygenated metabolite of cholesterol, is capable of diffusing into the bloodstream. The metabolism of brain cholesterol also generates nonsterol isoprenoids, which are required to activate the small GTP-binding proteins that regulate normal neuronal functions. Pathogenic huntingtin proteins inhibit the transcription of sterol regulatory element (SRE)-regulated gene products that are essential for cholesterol biosynthesis, resulting in a decreased concentration of plasma 24S-hydroxycholesterol—which has the potential to serve as a biomarker for disease progression[2].

Cholesterol dysregulation has also been reported in a variety of other neurodegenerative diseases including Alzheimer's disease, in which the plasma concentrations of 24S-hydroxycholesterol decrease as the disease progresses[8]. Amyloid-β oligomers, the causative proteins of Alzheimer's disease, have been shown to inhibit brain cholesterol synthesis[9]. Furthermore, an epidemiological study suggests an association between certain *CYP46A1* polymorphisms and a higher risk of Alzheimer's disease[10]. It has also been documented that hypercholesterolemia protects against amyotrophic lateral sclerosis, an adult-onset motor neuron disease[11]. Notably, mice lacking the liver X receptor-β, the receptor for 24S-hydroxycholesterol, show a progressive motor neuron degeneration[12].

These observations raise the intriguing possibility that disrupted cholesterol metabolism is closely related to the molecular underpinnings of various neurodegenerative diseases. However, it has yet to be clarified whether cholesterol itself, its metabolites or both have a major role in the maintenance of neuronal function. Moreover, it is also unclear whether augmenting brain cholesterol is capable of protecting debilitated neurons, given the detrimental effects of cholesterol, such as atherosclerosis.

Further basic research is necessary to understand how cholesterol dysregulation impairs neuronal functions and to identify therapies targeting cholesterol-dependent neuron damage. It is particularly important to develop methods to selectively manipulate cholesterol metabolism in the brain and to evaluate the effect and safety of such interventions.

1. Huntington, G. *Med Surg. Rep.* **26**, 317–321 (1872).
2. Leoni, V. *et al. Brain* **131**, 2851–2859 (2008).
3. Butler, R. & Bates, G. *Nat. Rev. Neurosci.* **7**, 784–796 (2006).
4. Katsuno, M. *et al. Nat. Med.* **9**, 768–773 (2003).
5. Valenza, M. *et al. J. Neurosci.* **25**, 9932–9939 (2005).
6. Valenza, M. *et al. Hum. Mol. Genet.* **16**, 2187–2198 (2007).
7. Kotti, T.J. *et al. Proc. Natl. Acad. Sci. USA* **103**, 3869–3874 (2006).
8. Shobab, L.A. *et al. Lancet Neurol.* **4**, 841–852 (2005).
9. Michikawa, M., Gong, J.S., Fan, Q.W., Sawamura, N. & Yanagisawa, K. *J. Neurosci.* **21**, 7226–7235 (2001).
10. Papassotiropoulos, A. *et al. Arch. Neurol.* **60**, 29–35 (2003).
11. Dupuis, L. *et al. Neurology* **70**, 1004–1009 (2008).
12. Andersson, S., Gustafsson, N., Warner, M. & Gustafsson, J.A. *Proc. Natl. Acad. Sci. USA* **102**, 3857–3862 (2005).

Neurobiology of Disease

Polyglutamine-Expanded Androgen Receptor Truncation Fragments Activate a Bax-Dependent Apoptotic Cascade Mediated by DP5/Hrk

Jessica E. Young,[1]* Gwenn A. Garden,[2,5]* Refugio A. Martinez,[1] Fumiaki Tanaka,[6] C. Miguel Sandoval,[6] Annette C. Smith,[1] Bryce L. Sopher,[1] Amy Lin,[7] Kenneth H. Fischbeck,[6] Lisa M. Ellerby,[7] Richard S. Morrison,[3,5] J. Paul Taylor,[8] and Albert R. La Spada[1,2,4,5]

Departments of [1]Laboratory Medicine, [2]Neurology, [3]Neurological Surgery, and [4]Medicine, and [5]Center for Neurogenetics and Neurotherapeutics, University of Washington, Seattle, Washington 98195-7110, [6]Neurogenetics Branch, National Institute of Neurological Disorders and Stroke–National Institutes of Health, Bethesda, Maryland 20892, [7]Buck Institute for Age Research, Novato, California 94945, and [8]Department of Neurology, University of Pennsylvania, Philadelphia, Pennsylvania 19104

Spinal and bulbar muscular atrophy (SBMA) is an inherited neuromuscular disorder caused by a polyglutamine (polyQ) repeat expansion in the androgen receptor (AR). PolyQ-AR neurotoxicity may involve generation of an N-terminal truncation fragment, as such peptides occur in SBMA patients and mouse models. To elucidate the basis of SBMA, we expressed N-terminal truncated AR in motor neuron-derived cells and primary cortical neurons. Accumulation of polyQ-AR truncation fragments in the cytosol resulted in neurodegeneration and apoptotic, caspase-dependent cell death. Using primary neurons from mice transgenic or deficient for apoptosis-related genes, we determined that polyQ-AR apoptotic activation is fully dependent on Bax. Jun N-terminal kinase (JNK) was required for apoptotic pathway activation through phosphorylation of c-Jun. Expression of polyQ-AR in DP5/Hrk null neurons yielded significant protection against apoptotic activation, but absence of Bim did not provide protection, apparently due to compensatory upregulation of DP5/Hrk or other BH3-only proteins. Misfolded AR protein in the cytosol thus initiates a cascade of events beginning with JNK and culminating in Bax-dependent, intrinsic pathway activation, mediated in part by DP5/Hrk. As apoptotic mediators are candidates for toxic fragment generation and other cellular processes linked to neuron dysfunction, delineation of the apoptotic activation pathway induced by polyQ-expanded AR may shed light on the pathogenic cascade in SBMA and other motor neuron diseases.

Key words: polyglutamine; spinal and bulbar muscular atrophy; truncation; apoptosis; Bax; DP5

Introduction

Spinal and bulbar muscular atrophy (SBMA), also known as Kennedy's disease, is an X-linked disorder characterized by progressive degeneration of motor neurons in the spinal cord and brainstem (Kennedy et al., 1968). The cause of SBMA is a trinucleotide (CAG) repeat expansion in the androgen receptor (AR) gene (La Spada et al., 1991). At least eight other disorders, including Huntington's disease (HD), dentatorubral-pallidoluysian atrophy, and six forms of spinocerebellar ataxia (SCA), result from this type of mutation (Zoghbi and Orr, 2000; Nakamura et al., 2001). SBMA is unique among the polyQ diseases because expression of the disease gene alone is not sufficient to produce the phenotype. Transgenic models of SBMA strongly suggest that females are protected by low levels of androgen (Katsuno et al., 2002; Chevalier-Larsen et al., 2004; Sopher et al., 2004), making SBMA a sex-limited disorder. Together with results from *Drosophila* and *in vitro* studies, it appears that polyQ AR neurotoxicity requires ligand binding (Darrington et al., 2002; Takeyama et al., 2002; Walcott and Merry, 2002; Pandey et al., 2007). When androgen binds to its receptor, AR is released from protein chaperones, dimerizes, and translocates to the nucleus where it binds DNA and activates gene expression. An androgen antagonist that blocks AR-mediated gene expression, but fails to prevent nuclear translocation, cannot prevent disease in fly and mouse models of SBMA (Katsuno et al., 2002; Takeyama et al., 2002). Thus, nuclear localization of polyQ-AR is likely a critical step in the pathogenic process (La Spada and Taylor, 2003; Sopher et al., 2004).

Several polyQ-expanded proteins undergo site-specific proteolysis that promotes the toxicity of the mutant protein (Miyashita et al., 1997; Kobayashi et al., 1998; Wellington et al., 1998). The resulting proteolytic fragments are observed in affected patients and mouse models of polyQ disease (Paulson et al., 1997; Li et al., 1998a; Schilling et al., 1999a,b; Garden et al., 2002). Such proteo-

Received Aug. 26, 2008; revised Nov. 26, 2008; accepted Dec. 31, 2008.

This work was supported by National Institutes of Health Grants NS41648 (A.R.L.), NS35533 (R.S.M.), NS40251A (L.M.E.), and NS53825 (J.P.T.); intramural National Institute of Neurological Disorders and Stroke funds (K.H.F.); and grants from the Muscular Dystrophy Association (A.R.L., J.P.T., and L.M.E.). We thank S. Finkbeiner, R. Youle, S. Gutkind, C. Duckett, E. Johnson, and G. Nunez for providing reagents or mice.

*J.E.Y. and G.A.G. contributed equally to this work.

Correspondence should be addressed to Dr. Albert R. La Spada, Department of Laboratory Medicine, University of Washington Medical Center, Box 357110, Room NW 120, Seattle, WA 98195-7110. E-mail: laspada@u.washington.edu.

J. P. Taylor's present address: St. Jude Children's Research Hospital, Memphis, TN 38105.

DOI:10.1523/JNEUROSCI.4072-08.2009

 0270-6474/09/291987-11$15.00/0

lytic fragments produce significant cellular toxicity in model systems, under conditions where full-length polyQ protein has little impact (Ikeda et al., 1996; Cooper et al., 1998; Ellerby et al., 1999a). PolyQ-expanded AR undergoes proteolytic modification *in vitro*, and polyQ-expanded N-terminal AR fragments are toxic to tissue culture cells, including neuronal cells (Kobayashi et al., 1998; Merry et al., 1998; Ellerby et al., 1999b). Furthermore, numerous studies of polyQ disease proteins have implicated caspase cleavage in the pathogenic cascade (Goldberg et al., 1996; Kobayashi et al., 1998; Wellington et al., 1998; Ellerby et al., 1999a,b). In HD, polyQ-huntingtin with a putative caspase-6 cleavage site mutation is incapable of causing neurotoxicity in transgenic mice (Graham et al., 2006). Thus, while a role for apoptotic mediators in polyQ disease pathogenesis seems likely, the cascade of molecular events leading to apoptotic activation in the various polyQ diseases remains unknown.

Here we define the pathway by which polyQ-AR elicits apoptotic activation in motor neuron-like cells and primary neurons. We show that neuronal expression of N-terminal truncated polyQ-AR elicits intrinsic pathway-mediated neuronal apoptosis, initiated by Jun N-terminal kinase (JNK) and culminating in Bax activation. The c-Jun-*N*-terminal kinases (JNKs) are a pro-apoptotic subgroup of mitogen-activated protein kinases that mediate neuronal apoptosis in response to a variety of stimuli, including activation of the unfolded protein response and proteasome impairment, both of which have been implicated as consequences of polyQ toxicity (Nishitoh et al., 2002; Morfini et al., 2006). A principal target of JNK is the transcription factor c-Jun, which is activated by phosphorylation within its transactivation domain, leading to increased expression of target genes that initiate the apoptotic cascade. Two BH3-only proteins, Bim and DP5/Hrk, are activated downstream of JNK and c-Jun in the initiation of neuronal apoptosis (Inohara et al., 1997; Imaizumi et al., 1999; Harris and Johnson, 2001; Putcha et al., 2001; Whitfield et al., 2001; Imaizumi et al., 2004), and one of these BH3-only proteins, DP5/Hrk, has been implicated in motor neuron degeneration (Shinoe et al., 2001; Imaizumi et al., 2004). In this study, we demonstrate, for the first time, a role for DP5/Hrk-mediated, Bax-dependent intrinsic pathway apoptotic activation, initiated by JNK, in the polyQ motor neuron disease SBMA.

Materials and Methods

Cell culture, primary neuron culture, and transfection. The AR-Q_N expression constructs and huntingtin exon-1/2-Q_N expression constructs (where N is the number of CAG repeats) have been described previously (Saudou et al., 1998; Taylor et al., 2003). MN-1 cells were cultured in 75 cm^2 vented tissue culture flasks at 37°C in a humidified atmosphere containing 5% CO_2 in DMEM (Invitrogen BRL) supplemented with 10% fetal bovine serum (v/v), 100 U/ml penicillin/100 μg/ml streptomycin and 2 mM L-glutamine. For Western blot and caspase activation assays, cells were seeded in six-well plates at a density of 300,000 cells per well at 24 h before transfection. We transfected MN-1 cells with 1 μg of plasmid DNA using Lipofectamine Plus following the manufacturer's protocol (Invitrogen). Cortical neurons were cultured from postnatal day 0 pups. Briefly, pups were decapitated into Hanks Media w/o Ca^{2+} and Mg^{2+}, and cortices were dissected in Neurobasal-A (NBA) media supplemented with B27 and L-glutamine. After dissection, cortices were trypsinized for 25 min at 37°C and dissociated. Cells were plated at a density of 2.5×10^5 per well in 4-well chamber CC2 slides (Nalge-Nunc). After 3 d, neurons were cultured in NBA media supplemented with B27 and L-glutamine, and were transfected using Lipofectamine 2000 following the manufacturer's protocol (Invitrogen). Use of B27 supplement, instead of serum, assures primary cultures consisting of at least 90% neurons. Primary neurons were subjected to taxol treatment by replacing media with taxol-containing media at a concentration of 250 nM. All experiments and animal care were performed in accordance with University of Washington IACUC guidelines.

Western blot analysis. Protein lysates were obtained by homogenizing cortices in sample buffer [160 mM Tris-HCl (pH 6.9), 4% SDS, 200 mM dithiothreitol, 20% glycerol, 0.004% Bromophenol blue] at a ratio of 1:10–1:20 (w/v). MN-1 cells were harvested by scraping in ice-cold lysis buffer (68 mM sucrose, 200 mM mannitol, 50 mM KCl, 1 mM EGTA, 1 mM EDTA, 1 mM DTT and 1× Complete Protease Inhibitor (Boehringer Mannheim). Cell membranes were disrupted with 80 strokes of a Wheaton dounce homogenizer (B-type pestle) and centrifuged at 4°C at 800 × *g*. The nuclear pellets were lysed in a buffer consisting of 150 mM NaCl, 6 mM Na_2HPO_4, 4 mM NaH_2PO_4, 1.2 mM EDTA, 1% NaDOC, 0.5% Triton-X, 0.1% SDS, and Complete Protease Inhibitor. Primary cortical neurons were harvested in radioimmunoprecipitation assay lysis buffer (10 mM Tris, 0.1% SDS, 1% SDOC, 0.01% TX-100, 150 mM NaCl) and homogenized by passing 5× through a 26.5 gauge syringe. Protein lysates (50 μg) were run on a 10% Bis-Tris gel (Invitrogen) and transferred to PVDF membranes (Millipore) using a semidry transfer system (Invitrogen). The membranes were blocked with 0.05% Tween 20, Tris-buffered saline (T-TBS) containing 5% nonfat dried milk at 4°C overnight, and then probed with phospho-c-Jun antibody (Ser63) II (1:1000, Cell Signaling), anti-AR N20 (1:1000, Santa Cruz), or anti-PUMA antibody (1:1000, Cell Signaling) in T-TBS containing 5% nonfat dried milk at room temperature (RT) for 1 h. After washing, membranes were incubated with HRP-conjugated anti-rabbit IgG (1:2000, Santa Cruz) in T-TBS for 1 h at RT. Blots were stripped and reprobed with mouse anti-actin antibody (1:5000, (Millipore Bioscience Research Reagents/Millipore), washed, and incubated in anti-mouse-HRP antibody (GE Healthcare). After treatment with ECL chemi-luminescence (NEN), the membranes were visualized by autoradiography. Band intensities were calculated using NIH ImageJ freeware. All immunoblots were performed in duplicate or triplicate.

FACS-assisted cell viability assay. At indicated time points, cells were harvested with trypsin, gently pelleted by centrifugation and resuspended in PBS with 1% serum on ice at a concentration 10^6/ml. The cells were stained with propidium iodide 1 μg/ml (PI, Sigma), gently vortexed, and incubated for 15 min at RT in the dark. 20,000 nongated events were acquired for each sample (Beckman Coulter FACS Calibur instrument; CellQuest software package for analysis). Results were expressed as a percentage of green fluorescent protein (GFP)/PI double-positive (nonviable, transfected) cells relative to total GFP positive (all transfected) cells.

Caspase assay. At the indicated time points, cells were harvested and lysed in 300 μl of buffer consisting of 10 mM Tris pH 7.3, 10 mM NaH_2PO_4, 150 mM NaCl, and 1% Triton X-100 and stored at −80°C. Caspase-3 activity was determined by incubating 100 μg of lysate with 50 μM fluorogenic substrate Ac-DEVD–AFC (Biosource International) in a total volume of 200 μl of assay buffer (20 mM HEPES, pH 7.4, 100 mM NaCl, 1 mM EDTA, 0.2% CHAPS, 20% glycerol, 10 mM DTT) in the dark for 2 h at 37°C. Substrate cleavage was detected using Cytofluor II Fluorescence multi-well plate reader (Perspective Biosystems) with excitation and emission wavelengths of 420 and 520 nm, respectively.

DNA laddering assay. To detect apoptosis-induced fragmentation of DNA, 10^6 cells were harvested and genomic DNA was extracted using the DNeasy Kit (Qiagen). Genomic DNA (500 ng) was ligated to 12-mer adapter oligonucleotides (ApoAlert LM-PCR Ladder Assay Kit, Clontech) as described in the manufacturer's protocol. Following ligation, samples were subjected to 15 – 20 cycles of PCR amplification (72°C for 8 min, followed by thermal cycling between 94°C for 1 min and 72°C for 3 min) using Advantage cDNA Polymerase Mix (Clontech). Reaction products were electrophoresed on a 1.5% agarose/ethidium bromide gel.

Immunocytochemistry and primary neuron toxicity assays. Neurons were fixed with 4% paraformaldehyde (PFA) for 10 min at RT, washed with PBS, counterstained with Hoescht dye, and coverslipped. For the toxicity studies, cells were fixed in 4% PFA, permeabilized with 0.25% Triton X-100, blocked with Pro-Block, then incubated overnight in rabbit anti-active caspase-3 (1:100, Cell Signaling) and mouse-anti MAP2 (1:200, Millipore Bioscience Research Reagents). Cells were then incubated in anti-rabbit 594 (1:1000, Invitrogen) and anti-mouse 647 (1:

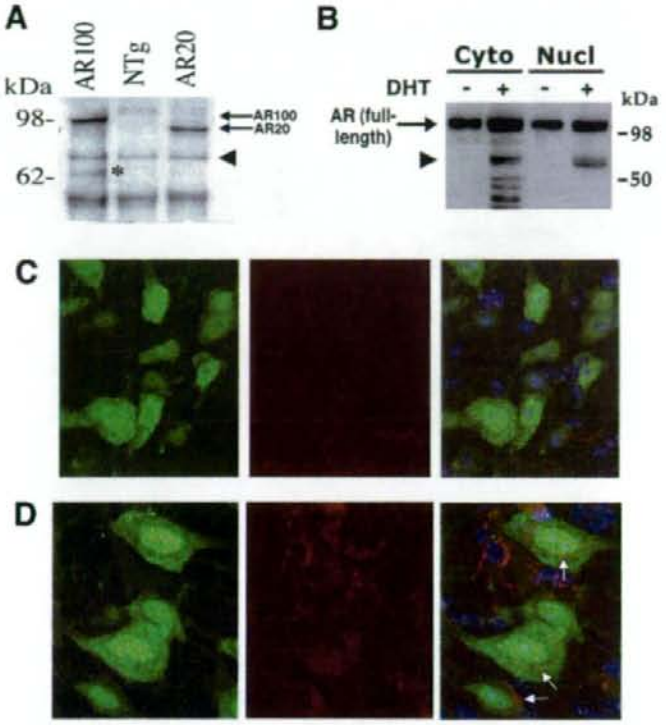

Figure 1. SBMA transgenic mice express an N-terminal AR truncation product in the cytosol. ***A***, Western blot analysis of cortex. Protein lysates from 12-month-old AR YAC CAG100 transgenic mice (AR100), nontransgenic littermates (NTg), and AR YAC CAG20 transgenic controls (AR20) were immunoblotted with AR antibody N20. Full-length AR100 and AR20 protein is detected (arrows). An ~65 kDa truncation product (asterisk) is detected in the AR100 mice, but no truncation fragment is present in the AR20 mice. Arrowhead indicates a cross-reactive band that serves as a loading control. The 65 kDa N-terminal truncation fragment in AR YAC CAG100 mice is also present in spinal cord lysates (data not shown). ***B***, Fractionation of AR truncation fragments. We transfected HEK293T cells with an AR112 expression construct and cultured the transfected cells in either the presence or absence of the AR ligand, dihydrotestosterone (DHT). Ligand binding elicited AR truncation that was more prominent in the cytosol (Cyto) than in the nucleus (Nucl), and arrowhead indicates an AR N-terminal truncation product of comparable size to the fragment detected *in vivo*. We confirmed integrity of the fractions by reprobing immunoblots with compartment-specific antibodies (data not shown). ***C***, ***D***, IHC analysis suggests accumulation of AR in perinuclear cytosol. Lumbar cord sections from 4-month-old nontransgenic mice (***C***) and AR YAC CAG100 transgenic mice (***D***) were stained with NeuN to label neurons (green; left), N-terminally directed anti-AR antibody N-20 (red; middle), and DAPI (blue). Perinuclear staining (arrows) is apparent in the merged images (right) of motor neurons in AR YAC CAG100 spinal cord sections (***D***), but not in nontransgenic controls (***C***). There was no perinuclear AR staining in AR YAC CAG20 transgenic mice (data not shown).

1000, Invitrogen) and counterstained with DAPI. Note that although GFP and AlexaFluor 647 (Cy5) labeling both appear green on fluorescent images, different filters allow us to differentiate them with four-channel imaging. For quantification of c-Jun-P positive neurons, we fixed neurons at 18 h after transfection and incubated overnight with anti-PhosphoSer73-c-Jun (1:1000, Cell Signaling). JNK Inhibitor II (Cal Biochem) was reconstituted in DMSO and added to primary neuron culture media to yield a final concentration of 10 μM (Donovan et al., 2002), while JNK Inhibitor III (Cal Biochem) was reconstituted in DMSO and added to primary neuron culture media to yield a final concentration of 5 or 20 μM (Holzberg et al., 2003). JNK Inhibitor-containing media or DMSO-only containing media was used to replace primary neuron culture media, and active caspase-3 and MAP2 immunoreactivity were measured 24 h after media replacement. Fluorescence was analyzed on a Zeiss inverted fluorescence microscope and image analysis was done with SLIDEBOOK software. All experiments were done in triplicate or quadruplicate, and ≥50 neurons were quantified per condition in each run.

RNA interference constructs. The lentiviral vector, pRRLsin-cppt-pgk-wpre-GFP (Add-gene plasmid #12252) was modified to express a short hairpin sequence targeting either the murine DP5 or Bim mRNA. Briefly, the WPRE promoter and GFP sequence were replaced with a CMV promoter and eCFP sequence from the plasmid pECFP-C1 (Clontech) by cloning into unique *XcmI* and *SalI* sites. The mouse U6 promoter and shRNA sequence were then PCR subcloned 5′ to the CMV/eCFP sequence.

Real-time RT-PCR. Cells were harvested and total RNA purified (Qiagen). Quantification of *DP5*, *Bim*, or *Puma* RNA expression in primary cortical neurons or Neuro2a cells was done, using murine-specific TaqMan Assay-on-Demand primers and probe (ABI), and normalizing to eukaryotic 18S ribosomal RNA, according to the manufacturers' instructions (ABI). All experiments were done in triplicate.

Statistical analysis. All errors bars shown in the Figures are SEM. All data were prepared for analysis with standard spreadsheet software (Microsoft Excel). Statistical analysis was done using Microsoft Excel or the VassarStats website (http://faculty.vassar.edu/lowry/VassarStats.html). For ANOVA analysis involving multiple sample comparisons, we performed *post hoc* testing to discriminate significance relationships.

Results

N-terminal truncation products occur in the cytosol in SBMA cells and motor neurons

We previously generated AR YAC CAG100 transgenic mice that strikingly recapitulate the late-onset, gender-dependent, neurogenic muscular atrophy phenotype of SBMA patients (Sopher et al., 2004). To determine whether an N-terminal AR truncation fragment is produced in this highly representative SBMA mouse model, we performed Western blot analysis on brain protein lysates obtained from presymptomatic AR YAC CAG100 transgenic mice and age-matched AR YAC CAG20 and nontransgenic controls. Immunoblotting with an anti-AR antibody, directed against the N terminus, revealed an ~65 kDa truncation fragment in AR YAC CAG100 mice, but no truncation fragment was detected in AR YAC CAG20 mice (Fig. 1*A*). Fractionation of HEK293T cells expressing AR112 protein revealed that proteolytic cleavage of AR is ligand-dependent, and that an N-terminal fragment of ~65 kDa is present in the cytosol as well as the nucleus (Fig. 1*B*). To establish whether the N-terminal truncated AR protein was expressed in motor neurons, we performed immunohistochemistry (IHC) upon lumbar spinal cord sections from SBMA AR100 mice, and detected AR protein in motor neuron perinuclear cytosol (Fig. 1*C*,*D*), and nuclei (Sopher et al., 2004), with an antibody that recognizes the N-terminal region of AR. Immunostaining with a C-terminally directed anti-AR antibody, however, did not reveal immunoreactivity in the perinuclear cytosol (data not shown). This observation is consistent with a recent study of a different SBMA mouse model in which insoluble, polyQ-expanded AR protein derived from brain extract consisted of a similarly sized N-terminal truncated AR protein (Li et al., 2007).

In that study, the production of N-terminal AR truncation fragments correlated with neurological disease progression (Li et al., 2007).

Truncated polyQ-expanded AR induces apoptosis in MN-1 cells and in primary neurons

In light of the evidence for the production and pathogenic nature of N-terminal truncated AR protein, we engineered AR expression constructs, terminating within a region of putative proteolytic cleavage (Ellerby et al., 1999b), to approximate the size of the N-terminal AR fragments observed in SBMA patient tissue and SBMA mice, and tagged them with GFP (supplemental Fig. 1, available at www.jneurosci.org as supplemental material). Transfection of N-terminal truncated AR expression constructs into the motor neuron-derived cell line, MN-1, yielded polyQ length-dependent toxicity (Fig. 2*A*). The toxicity induced by polyQ-expanded AR was readily observed by fluorescence microscopy, as cells transfected with polyQ-expanded AR became progressively rounded and ultimately lifted off the bottom of the flask. Examination of living cells, transfected with Nt-AR112-GFP and stained with Hoechst 33342, revealed numerous inclusion-containing cells with condensed, fragmented nuclei (data not shown). To verify that polyQ-expanded AR toxicity in culture was leading to apoptotic cell death, we examined transfected MN-1 cells for evidence of endonuclease-mediated laddering of chromosomal DNA and activation of caspase-3, two biochemical hallmarks of apoptotic cell death. MN-1 cells expressing Nt-AR112-GFP displayed DNA laddering that was first detectable 48 h after transfection, and peaked 96 h after transfection (Fig. 2*B*). Induction of DNA laddering did not occur after transfection of Nt-AR19-GFP, indicating that apoptotic activation was polyQ length-dependent (Fig. 2*B*). Apoptotic cell death is consummated in large part by activation of the caspase cascade. Caspase-3 is an executioner caspase whose ultimate activation may be elicited by a wide variety of toxic insults (Stennicke and Salvesen, 1998). Transfection of MN-1 cells with Nt-AR112-GFP yielded polyQ length-dependent activation of caspase-3, with a peak ~72 h, correlating well with the time course of DNA laddering and loss of cell viability (Fig. 2*C*).

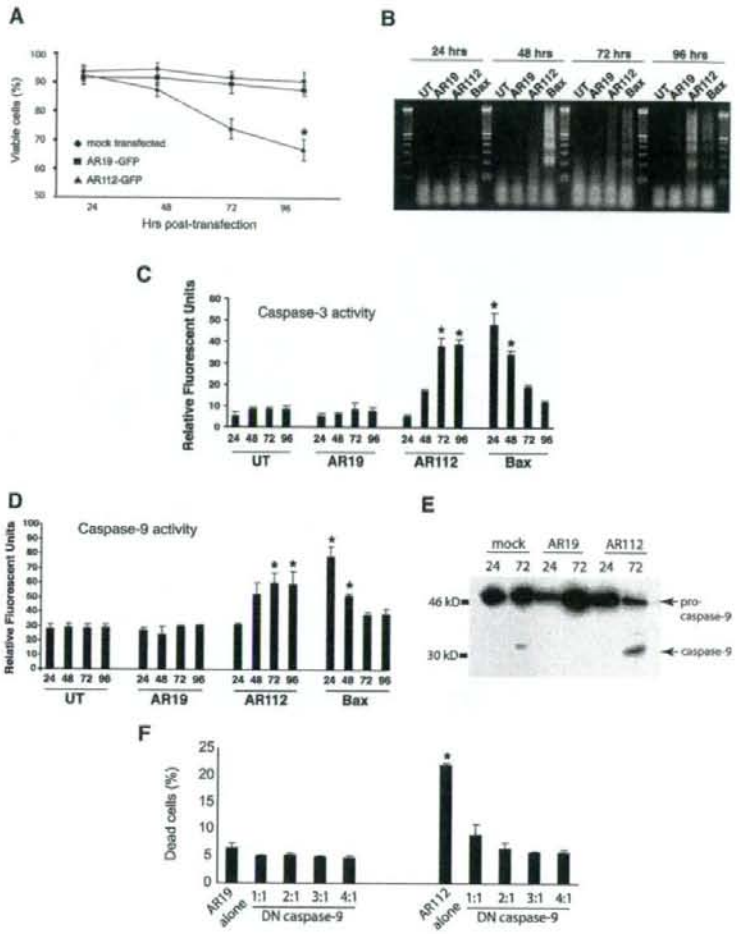

Figure 2. Expression of N-terminal polyQ AR fragment in MN-1 cells induces caspase-mediated apoptosis via intrinsic pathway. ***A***, FACS-assisted cell viability assay demonstrates polyQ length-dependent cytotoxicity of N-terminal AR fragment (*$p < 0.01$; Student's *t* test). ***B***, AR112 truncation fragment induces apoptotic nuclear fragmentation, reaching a peak at 96 h after transfection. Bax induces nuclear fragmentation with more rapid kinetics, peaking at 48 h. Untransfected (UT) cells and AR19-transfected cells do not show nuclear fragmentation. ***C***, AR112 truncation fragment induces caspase-3 activation reaching a peak at 72 h after transfection (*$p < 0.01$; Student's *t* test). Bax induces caspase-3 activation with more rapid kinetics, peaking at 24 h. ***D***, Fluorogenic substrate assay demonstrates activation of caspase-9 in AR112-transfected MN-1 cells peaking 72 h after transfection (*$p < 0.01$; Student's *t* test). Caspase-9 is activated in Bax-transfected cells peaking 24 h after transfection. ***E***, Western blot analysis reveals prominent cleavage of pro-caspase-9 in AR112-transfected cells 72 h after transfection to yield considerable generation of active caspase-9. ***F***, Dominant-negative caspase-9 expression rescues polyQ-length-dependent toxicity of N-terminal truncated AR112. MN-1 cell death, as measured by propidium iodide uptake, is significantly improved when dominant negative caspase-9 is cotransfected with the AR112 truncation fragment (*$p < 0.01$; Student's *t* test).

To explore the pathway upstream of caspase-3 activation, we measured the activity of two initiator caspases, caspase-8 and caspase-9, using specific fluorogenic substrates. Nt-AR112-GFP led to activation of caspase-9, but not caspase-8 (Fig. 2*D*; supplemental Fig. 2, available at www.jneurosci.org as supplemental material). Consistent with these observations, we found that the caspase-9 inhibitor zLEHD-fmk attenuated caspase-3 activation following transfection of MN-1 cells with Nt-AR112-GFP, but the caspase-8 inhibitor zIETD-fmk did not (data not shown). Activation of caspase-9 in the setting of truncated AR112 toxicity was further confirmed by Western blot analysis, which revealed that a 48 kDa pro-caspase-9 precursor was processed into the active caspase-9 fragment (Fig. 2*E*). When we coexpressed a dominant negative version of caspase-9 (Richter et al., 2001), we observed a marked reduction in toxicity in MN-1 cells expressing Nt-AR112-GFP (Fig. 2*F*), further confirming that caspase-9 was mediating AR polyQ length-dependent apoptotic cell death.

To examine the toxicity of N-terminal truncated polyQ-expanded AR fragment in postmitotic neurons, we derived primary mouse cortical neurons from neonatal C57BL/6J pups and,

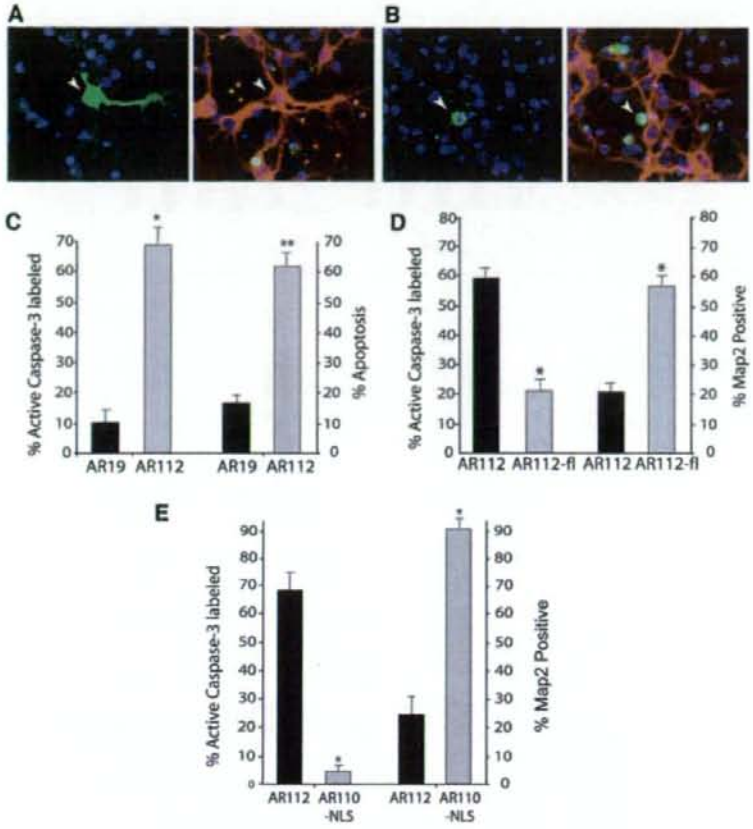

Figure 3. Expression of AR truncation fragment in the cytosol results in neurite degeneration and apoptotic cell death in a primary cortical neuron model of AR-polyQ neurotoxicity. ***A***, ***B***, Here, we see representative images of AR-transfected neurons using four-channel imaging: DAPI (blue), GFP (green, left), Cy3-labeled MAP2 (red), and Cy5-labeled active caspase-3 (green, right). ***A***, Transfection of AR19 does not cause toxicity. Left, Here we see GFP-tagged AR19 expression in a transfected neuron (arrowhead), demonstrating the presence of AR in the cytosol and neuritic processes. Right, Labeling of MAP2 (red) reveals normal, healthy neurites in the AR19-expressing neuron, and a nucleus that lacks caspase-3 activity (green). ***B***, Transfection of AR112 produces neurotoxicity. Left, Neuron expressing GFP-tagged AR112 (arrowhead) displays nuclear condensation and fragmentation. Right, AR112-expressing cortical neuron displays no MAP2 staining (red), but does label positive for active caspase-3 (green). ***C***, Comparison of AR19-expressing cortical neurons to AR112-expressing cortical neurons reveals marked caspase-3 activation and frequent apoptotic nuclear morphology in neurons expressing polyQ-expanded AR (*$p < 0.01$, **$p < 0.001$; ANOVA). ***D***, Primary neurons were transfected with Nt-AR112-GFP (AR112) or with the GFP-tagged full-length AR112 (AR112-fl). Primary neurons were cultured in 10 μM DHT to permit ligand activation of AR112-fl. Quantification of caspase-3 activation and MAP immunoreactivity indicates that AR112-fl does not produce significant neurotoxicity (*$p < 0.05$; ANOVA). All results were obtained at 24 h after transfection for ***A–E***. ***E***, Targeting polyQ-expanded, N-terminal truncated AR to the nucleus does not produce caspase activation, cell death, or neurite degeneration at 48 h after transfection (*$p < 0.01$; ANOVA). There was also no toxicity at 24 h after transfection (data not shown).

using standard lipofection, we transfected primary cortical neurons with Nt-AR19-GFP and Nt-AR112-GFP CMV expression constructs. GFP tagging allowed us to track the fate of individual cortical neurons expressing truncated AR protein products. Using this approach, we found that truncated AR112 accumulated in the perinuclear cytosol, while truncated AR19 was diffusely distributed throughout the cytosol and neurite processes (Fig. 3*A*,*B*). Cortical neurons expressing Nt-AR112-GFP demonstrated nuclear condensation, loss of microtubule-associated protein 2 (MAP2) staining, and caspase-3 activation, all by 24 h after transfection (Fig. 3*B*,*C*). These findings suggested a polyQ length-dependent induction of apoptotic cell death, as we found that nuclear morphological changes indicative of cell death correlated with caspase-3 activation for ~98% of assayed neurons (data not shown). When we expressed full-length AR112 in primary cortical neurons, we did not observe appreciable neurite degeneration or apoptotic cell death at 24 h after transfection in the presence of dihydrotestosterone, an AR ligand that favors translocation into the nucleus (Fig. 3*D*). Hence, nuclear localization was observed, and although neurite degeneration and apoptotic cell death did ultimately occur at 60 h after transfection, this was only after polyQ-expanded AR had relocalized to the cytosol (data not shown). To confirm that localization to the cytosol is required for neurite degeneration and apoptotic cell death, we fused a nuclear localization signal (NLS) to the N terminus of the truncated AR coding sequence. Cortical neurons transfected with NLS-AR110 showed nuclear accumulation of AR protein, but did not display neurite degeneration or apoptotic cell death, unlike cortical neurons transfected with unmodified truncated AR112 expression constructs (Fig. 3*E*).

The Bcl-2 family of apoptosis regulators mediates AR112-induced neuronal apoptosis

Activation of caspase-9 is mediated by the intrinsic pathway in which increased mitochondrial membrane permeability is induced by changes in the bioenergetics state of the cell, shifts in Ca^{2+} concentration, or alterations in the ratio of pro-apoptotic to anti-apoptotic members of the Bcl-2 family of proteins (Li et al., 1997; Yuan and Yankner, 2000). The release of pro-apoptotic factors, including cytochrome *c* and Smac/Diablo, from the mitochondrial intermembrane space promotes the formation of the Apaf-1 apoptosome that cleaves pro-caspase-9. Selective activation of caspase-9 by polyQ-expanded AR suggested that apoptosis was mediated by the intrinsic pathway. This hypothesis was supported by the observation that overexpression of Bcl-2 markedly ameliorated the toxicity of Nt-AR112-GFP in MN-1 cells (Fig. 4*A*). To determine whether Nt-AR112-GFP toxicity in primary neurons also involved the intrinsic pathway, we obtained transgenic mice overexpressing *Bcl-2* under the control of the neuron specific enolase promoter (Martinou et al., 1994). We transfected primary cortical neurons from Bcl-2 overexpressing mice or from wild-type littermate controls with Nt-AR112-GFP. Bcl-2 overexpression provided nearly complete protection from AR112 neurotoxicity (Fig. 4*B*), suggesting that neurodegeneration in this model is mediated by activation of pro-apototic Bcl-2 family members. The pro-apoptotic Bcl-2 family member Bax mediates neuronal apoptosis in response to a wide variety of stimuli, and